HOXC13 promotes cell proliferation, metastasis and glycolysis in breast cancer by regulating DNMT3A

HONGRUI LI[1,2], PENGCHENG GAO[1,2], HAIFENG CHEN[1,2], JUNJIE ZHAO[1,2], XIANGZHONG ZHANG[1,2], GANGGANG LI[1,2], LITING WANG[1,2] and LONG QIN[1,2]

[1]Department of Thyroid and Breast Diseases, Jincheng People's Hospital; [2]Department of Thyroid and Breast Diseases, Jincheng Hospital Affiliated to Changzhi Medical College, Jincheng, Shanxi 048000, P.R. China

Received January 12, 2023; Accepted April 25, 2023

DOI: 10.3892/etm.2023.12138

Abstract. Breast cancer (BC) is a life-threatening malignant tumor that affects females more commonly than males. The mechanisms underlying BC proliferation, metastasis and glycolysis require further investigation. Homeobox C13 (HOXC13) is highly expressed in BC; however, the specific mechanisms in BC are yet to be fully elucidated. Therefore, the aim of the present study was to investigate the role of HOXC13 in BC proliferation, migration, invasion and glycolysis. In the present study, the UALCAN database was used to predict the expression levels of HOXC13 in patients with BC. Western blot analysis and reverse transcription-quantitative PCR were used to determine the expression levels of HOXC13 in BC cell lines. Moreover, HOXC13 knockdown was induced using cell transfection, and the viability, proliferation and apoptosis of cells were detected using Cell Counting Kit-8, 5-ethynyl-2'-deoxyuridine staining and flow cytometry. Migration, invasion and epithelial-mesenchymal transition (EMT) were measured using wound healing assay, Transwell assay and western blotting. In addition, XF96 extracellular flux analyzer and corresponding kits were used to detect glycolysis. The JASPAR database was used to predict promoter binding sites for the transcription factors HOXC13 and DNA methyltransferase 3α (DNMT3A). HOXC13 expression was silenced and DNMT3A was simultaneously overexpressed using cell transfection. The results of the present study revealed that HOXC13 expression was significantly elevated in BC tissues and cells. Following HOXC13 knockdown in BC cells, the viability, proliferation, glycolysis, migration, invasion and EMT were significantly decreased, and apoptosis was significantly increased. In addition, HOXC13 positively regulated the transcription of DNMT3A in BC cells, thus playing a regulatory role in the malignant progression of cells. In conclusion, HOXC13 promoted cell viability, proliferation, migration, invasion, EMT and glycolysis in BC by regulating DNMT3A.

Correspondence to: Dr Long Qin, Department of Thyroid and Breast Diseases, Jincheng People's Hospital, 456 Wenchang East Street, Jincheng, Shanxi 048000, P.R. China
E-mail: ql382721976@163.com

Key words: breast cancer, homeobox C13, DNA methyltransferase 3α, proliferation, metastasis, glycolysis

Introduction

Breast cancer (BC) is a malignant tumor with high incidence rates in female patients, which impacts both health and quality of life (1). According to data released by the International Agency for Research on Cancer, part of the World Health Organization, there were 2.26 million new cases of BC and 680,000 deaths worldwide in 2020 (2). The number of new cases of BC in China was 420,000, resulting in ~120,000 deaths. Notably, an aging population increases the overall risk of BC (3).

Glucose metabolism in tumor cells is characterized by increased glucose uptake and aerobic glycolysis. Since aerobic glycolysis occurs in cancer cells, the efficiency of sugar utilization is notably higher than that of healthy cells. Despite sufficient oxygen, cancer cells use aerobic glycolysis to produce energy (4). Aerobic glycolysis plays a fundamental role in cytoskeletal remodeling and cell motility in BC (5). In addition, aerobic glycolysis promotes the migration and proliferation of BC cells, and inhibits apoptosis (6). These results indicate that aerobic glycolysis serves an important role in BC cells.

Homeobox (HOX) genes are highly conserved at the genomic level, and play a key role in the regulation of numerous biological processes, including apoptosis, cell differentiation, transfer and receptor signal transduction (7). As a member of the HOX gene family, HOXC13 is a homologous box gene and is a key transcription factor for the growth and development of mammals (8). A previous study demonstrated that HOXC13 expression is higher in BC than in gastric, colon and other types of cancer, and results of a survival analysis demonstrated that high expression levels of HOX transcript antisense RNA and HOXC13 are associated with a poor prognosis (9). However, the role of HOXC13 in BC is yet to be fully elucidated. Notably, HOXC13 can promote the proliferation of esophageal squamous cell carcinoma by inhibiting caspase 3 transcription (10). In addition, when compared with healthy tissue, HOXC13 mRNA expression levels are increased in lung cancer tissue. HOXC cluster antisense RNA 2 (HOXC-AS2)

overexpression has been reported to significantly activate HOXC13 protein and mRNA expression, and HOXC-AS2 gene knockdown can inhibit the proliferation and migration of lung cancer cells (11). In addition, HOXC13 knockdown reverses the increased proliferation and migration of lung cells (11). HOXC13 can also promote cervical cancer cell proliferation and invasion, and the Warburg effect via the β-catenin/c-Myc signaling pathway (12). Thus, it was hypothesized that HOXC13 may serve a role in the proliferation, migration and glycolysis of BC.

DNA methyltransferase 3α (DNMT3A) is highly expressed in a variety of malignant tumors and is a key enzyme required for the re-methylation of mammalian genes. DNMT3A may serve as a potential therapeutic target in the prevention of cancer recurrence (13,14). Downregulated DNMT3A expression decreases the Warburg effect, proliferation and invasion of ovarian cancer cells (15). In addition, DNMT3A promotes colorectal cancer progression by regulating DOC-2/DAB2 interactive protein-mediated MEK/ERK activation (16). Upregulated DNMT3A expression promotes progression of BC (17). However, the regulatory association between HOXC13 and DNMT3A in BC, and the regulatory effects of DNMT3A on BC cell proliferation, invasion and glycolysis are yet to be fully elucidated.

Thus, the present study knocked down HOXC13 and overexpressed DNMT3A concurrently to determine the roles of HOXC13 and DNMT3A in BC, and the underlying regulatory mechanisms in BC cell proliferation, invasion and glycolysis.

Materials and methods

The application of UALCAN and JASPAR databases. The UALCAN database based on The Cancer Genome Atlas was used to predict HOXC13 expression in patients with BC (18). The JASPAR database was used to predict promoter binding sites for the transcription factors HOXC13 and DNMT3A (19).

Cell culture. The human BC cell lines MCF-7 (cat. no. TCHu 74), BT-549 (cat. no. TCHu 93) and MDA-MB-231 (cat. no. TCHu227) were purchased from The Cell Bank of Type Culture Collection of The Chinese Academy of Sciences. Human mammary epithelial MCF-10A cells (cat. no. BNCC337734) were purchased from BeNa Culture Collection (Beijing Beina Chunglian Institute of Biotechnology). Cells were cultured in DMEM (Gibco; Thermo Fisher Scientific, Inc.) supplemented with 10% fetal bovine serum (FBS; Gibco; Thermo Fisher Scientific, Inc.) at 37˚C in a humidified atmosphere containing 5% CO_2.

Reverse transcription-quantitative PCR (RT-qPCR). Total RNA was isolated from human mammary epithelial MCF-10A cells and human BC cells using TRIzol® reagent (Invitrogen; Thermo Fisher Scientific, Inc.) and reverse-transcribed into cDNA using the PrimeScript RT Reagent kit (Takara Bio, Inc.), according to the manufacturer's protocol. qPCR was performed using the SYBR Green kit (Takara Bio, Inc.) on the ABI 7500 Real-Time PCR System (Applied Biosystems; Thermo Fisher Scientific, Inc.). Thermocycling conditions were as follows: Initial denaturation for 5 min at 95˚C, followed by 40 cycles of 15 sec at 95˚C and 34 sec at 60˚C and extension at 72˚C for 30 sec, with a final extension step at 72˚C for 10 min. GAPDH was used as the internal control and expression levels were calculated using the $2^{-\Delta\Delta Cq}$ method (20). The sequences of primers used for RT-qPCR were as follows: HOXC13 forward, 5'-CCATAACCGAACCCACGGAA-3' and reverse, 5'-AATTGGGGCCATTCGGGATT-3'; DNMT3A forward, 5'-GGCCATACGGTGGAGCC-3' and reverse, 5'-TGTTGAGCCCTCTGGTGAAC-3' and GAPDH forward, 5'-AATGGGCAGCCGTTAGGAAA-3' and reverse, 5'-GCGCCCAATACGACCAAATC-3'.

Western blot analysis. Total cellular protein was extracted using RIPA lysis buffer (Beyotime Institute of Biotechnology) on ice. The total protein concentration was measured with a BCA protein assay kit (Takara Biotechnology Co., Ltd.). A total of 30 μg/lane protein was separated by SDS-PAGE on 10% gels and transferred onto PDVF membranes (MilliporeSigma) that were then blocked with 5% BSA for 2 h at room temperature. The following antibodies were added and incubated at 4˚C overnight: Anti-HOXC13 (1:1,000; cat. no. ab168368; Abcam), anti-E-cadherin (1:1,000; cat. no. ab40772; Abcam), anti-N-cadherin (1:1,000; cat. no. ab76011; Abcam), anti-Vimentin (1:1,000; cat. no. ab92547; Abcam), anti-hexokinase II (HK2; 1:1,000; cat. no. ab209847; Abcam), anti-pyruvate kinase M2 (PKM2; 1:1,000; cat. no. ab85555; Abcam), anti-DNMT3A (1:1,000; cat. no. ab188470; Abcam) and anti-GAPDH (1:1,000; cat. no. ab8245; Abcam). Horseradish peroxidase-conjugated anti-rabbit IgG antibody (1:5,000; cat. no. ab288151; Abcam) or anti-mouse IgG antibody (1:2,000; cat. no. ab6728; Abcam) was added and incubated at 4˚C overnight. Protein bands were visualized using an enhanced chemiluminescence (ECL)-Plus kit (Thermo Fisher Scientific, Inc.). Blots were analyzed using ImageJ software (1.42q; National Institutes of Health).

Cell transfection. Cells were placed into 6-well plates until they reached 70-80% confluence. Small interfering (si) RNAs targeting HOXC13 (si-HOXC13#1 and si-HOXC13#2) and the corresponding negative control (NC; si-NC) were purchased from GeneChem, Inc.; the sequences were as follows: si-HOXC13#1 sense, 5'-UUAACAUUAAAUACUCUUCUG-3' and antisense, 5'-GAAGAGUAUUUAAUGUUAAGG-3'; si-HOXC13#2 sense, 5'-UCCUUAACAUUAAAUACUCUU-3' and antisense, 5'-GAGUAUUUAAUGUUAAGGAAA-3' and si-NC sense, 5'-UUCUCCGAACGUGUCACGUTT-3' and antisense, 5'-ACGUGACACGUUCGGAGAATT-3'. pcDNA3.1 vectors containing full-length HOXC13 gene were used and empty pcDNA3.1 vectors (Shanghai GenePharma, Co., Ltd.) were used as the negative control. pcDNA3.1 containing HOXC13 (Oe-HOXC13) and DNMT3A (Oe-DNMT3A) and the corresponding NC plasmid (Oe-NC) were synthesized by Shanghai GenePharma, Co., Ltd. Transfection with aforementioned plasmids and siRNAs at a final concentration of 10 nM was performed using Lipofectamine® 2000 (Invitrogen; Thermo Fisher Scientific, Inc.) at 37˚C for 48 h, according to the manufacturer's instructions and the transfection was completed. Further experiments were performed after 48 h.

Cell Counting Kit (CCK)-8. Transfected BC cells were seeded in 96-well plates at the density of $5x10^3$ cells/well. After 24, 48 and 72 h of culture, CCK-8 solution (cat. no. ab228554; Abcam) was added to each well for 2 h at 37˚C, according to the manufacturer's instructions. The absorbance in each well was measured using a microplate reader at 450 nm.

5-ethynyl-2'-deoxyuridine (EdU) staining. Cell proliferation was determined via uptake of EdU into DNA using a Click-iT EdU Microplate Assay kit (Invitrogen; Thermo Fisher Scientific, Inc.), according to the manufacturer's instructions. Cells were seeded into 96-well plates ($3x10^3$ cells/well) and 10 μl EdU solution was added to each well for 18 h at 37˚C. Following nuclear staining with DAPI for 30 min at room temperature, cells were visualized under a BZ-8000 fluorescence microscope (Keyence Corporation).

Apoptosis assay. The apoptosis of cells was assessed via Annexin V-FITC/PI staining (Invitrogen; Thermo Fisher Scientific, Inc.) and flow cytometry, according to the manufacturer's instructions. The cells were washed with PBS and the cell concentration was adjusted to $7x10^4$ cells/ml. Cells were resuspended in 500 μl binding buffer containing 5 μl Annexin V-FITC and 5 μl PI (Invitrogen; Thermo Fisher Scientific, Inc.). Samples were incubated at 4˚C for 15 min in the dark and analyzed using BD FACSAria flow cytometry (BD Biosciences) with excitation at 488 nm and emission measured at 560 nm. Data were analyzed using CellQuest 16.0 software (BD Biosciences).

Transwell assay. The Transwell assay was conducted using a Transwell chamber coated with Matrigel (pore size, 8 μm; BD Biosciences) for 30 min at 37˚C. A total of $2x10^4$ cells in serum-free medium were plated in the upper chambers, and medium containing 20% FBS was added to the lower chambers. After 24 h at 37˚C, cells in the upper chambers were removed, and remaining cells were fixed with 4% methanol for 40 min at 4˚C. After staining with 0.1% crystal violet at room temperature for 30 min, migrated cells were visualized under a light microscope and counted using ImageJ software (1.42q; National Institutes of Health).

Wound healing assay. Cells were plated in 6-well plates at $1x10^5$ cells/well using serum-free DMEM at 37˚C for 24 h until cells reached 90% confluence. Linear wounds were created using a 200-μl pipette tip and cells were incubated overnight at 37˚C with 5% CO_2. Wounds were imaged at 0 and 24 h under a light microscope. Cell migration rate=(0 h scratch width-scratch width after culture)/0 h scratch width x100.

Extracellular acidification rate (ECAR) assay. Seahorse XF96 Extracellular Flux Analyzer (Seahorse Bioscience) was used for measuring ECAR. Cells (density, $1x10^5$) were plated in XF96 cell culture plates (Seahorse Bioscience) and incubated at 37˚C for 8 h. Following the addition of glucose, oligomycin (oxidative phosphorylation inhibitor) and 2-DG (glycolytic inhibitor), cells were equilibrated with bicarbonate-free buffered DMEM (Gibco; Thermo Fisher Scientific, Inc.) for 1 h at 37˚C without CO_2, immediately before the extracellular flux assay.

3-bromopyruvate (3BP; Sigma-Aldrich; Merck KGaA) solution in assay medium (final concentration, 10X; Gibco; Thermo Fisher Scientific, Inc.) was loaded into the sensor cartridge (final concentration, 20 or 100 μM). The instrument was set to acquire consecutive measurements for 1 h with mixing. 3BP was injected after acquiring one measurement as the baseline ECAR.

Lactic acid measurement. A lactic acid assay kit (cat. no. A019-2-1; Nanjing Jiancheng Bioengineering Institute) was used to measure lactic acid production, according to the manufacturer's instructions. Cells were counted directly using ImageJ software (1.42q; National Institutes of Health) for data normalization and to determine the final amount of lactate production.

Glucose consumption. Glucose consumption was determined using a Glucose Assay kit (Sigma-Aldrich; Merck KGaA), according to the manufacturer's instructions. Cells were seeded in a 96-well plate (density, $1x10^4$) in serum-free DMEM (Gibco; Thermo Fisher Scientific, Inc.) and 10 μl/well 2-deoxy-d-glucose was added at 37˚C for 30 min. A total of 50 μl/well 2-deoxy-d-glucose uptake assay working solution was added and cells were incubated at room temperature for 90 min. The optical density ratio at 570/610 nm was measured using a spectrophotometer (Thermo Fisher Scientific, Inc.).

Luciferase reporter assay. DNA fragments containing wild-type (WT) or mutant sequences for HOXC13 binding were synthesized and cloned into luciferase reporter vectors (pGL3-Basic; Addgene, Inc.). DNMT3A wild-type or mutant plasmids and Oe-HOXC13 or Oe-NC were co-transfected into cells using Lipofectamine 3000 (Invitrogen; Thermo Fisher Scientific, Inc.) for 48 h, according to the manufacturer's protocol. Transfected cells ($1x10^5$ per well) were seeded into 96-well plates and luciferase activity was determined 48 h after transfection using Dual-Luciferase® Reporter (DLR™) Assay System (Promega Corporation), according to the manufacturer's instructions. Firefly luciferase activity was normalized to *Renilla* luciferase activity.

Chromatin immunoprecipitation (ChIP). A ChIP assay was performed using a EZ-Magna ChIP A/G kit (cat. no. 17-10086; Merck KGaA). DNA and protein were cross-linked in 1% formaldehyde for 10 min at 37˚C, extracted using 300 μl SDS lysis buffer (EMD Millipore) and lysed using sonication (20 kHz; 4 pulses of 12 sec each, followed by 30 sec rest on ice between each pulse). Anti-HOXC13 antibody (1:100; cat. no. ab168368; Abcam) and IgG antibody (1:100; cat. no. ab90285; Abcam) were used for incubation with the supernatants. Following purification of the precipitated DNA, RT-qPCR was performed as aforementioned and the same primer pairs were used as those used for qPCR.

Statistical analysis. All data were analyzed using SPSS software (version 26.0; IBM Corp.) and are presented as the mean ± standard deviation. All experiments were performed in triplicate. Unpaired Student's t-test was used for comparison between two groups and one way-ANOVA followed by Tukey's post hoc test was used for comparison between

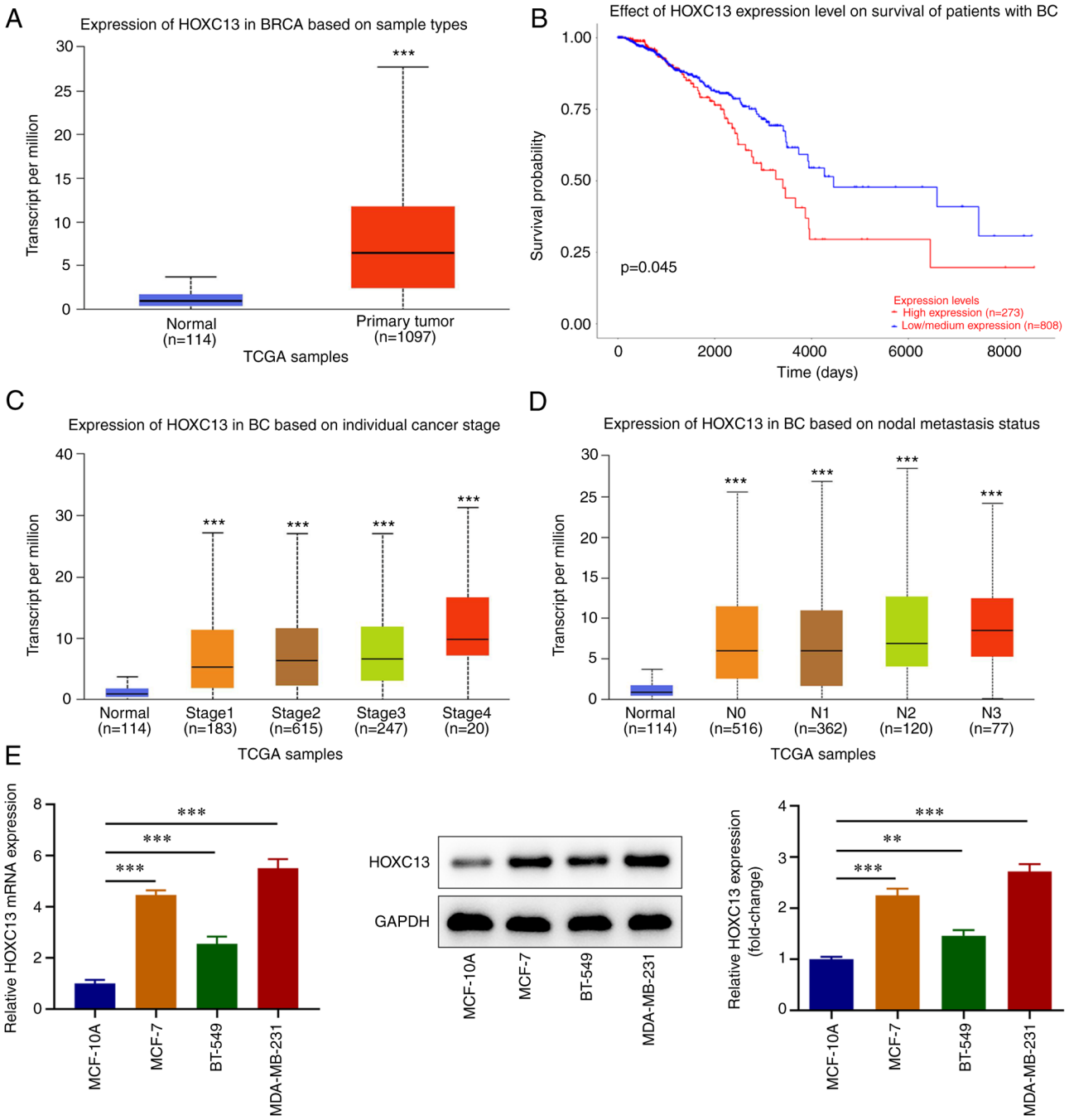

Figure 1. HOXC13 is highly expressed in BC. UALCAN database predicted (A) HOXC13 expression in patients with BC, and its association with (B) poor prognosis, (C) tumor stage and (D) regional lymph node involvement. (E) Reverse transcription-quantitative PCR and western blot analysis detected HOXC13 expression in BC cell lines. **P<0.01 and ***P<0.001 vs. normal or MCF-10A. HOXC13, homeobox C13; BC, breast cancer; TCGA, The Cancer Genome Atlas.

multiple groups. Survival analysis was performed using the Kaplan-Meier method. P<0.05 was considered to indicate a statistically significant difference.

Results

HOXC13 is highly expressed in BC. The UALCAN database demonstrated that HOXC13 expression was significantly increased in the tissues of patients with BC compared with the normal tissues from healthy individuals (Fig. 1A) and high HOXC13 expression in BC based on the criteria (Cutoff-High, median 50% and Cutoff-Low, median 50%) was associated with a poor prognosis (Fig. 1B). In addition, HOXC13 expression in BC was associated with tumor stage (Fig. 1C) and regional lymph node involvement (Fig. 1D). RT-qPCR and western blot analysis demonstrated that HOXC13 expression in BC cell lines was significantly increased compared with that in MCF-10A cells (Fig. 1E). HOXC13 expression was highest in MDA-MB-231 cells; thus, these were selected for use in subsequent experiments. In summary, HOXC13 displayed increased expression in BC tissues and cells.

HOXC13 knockdown inhibits the viability, proliferation and induces apoptosis of BC cells. HOXC13 knockdown was

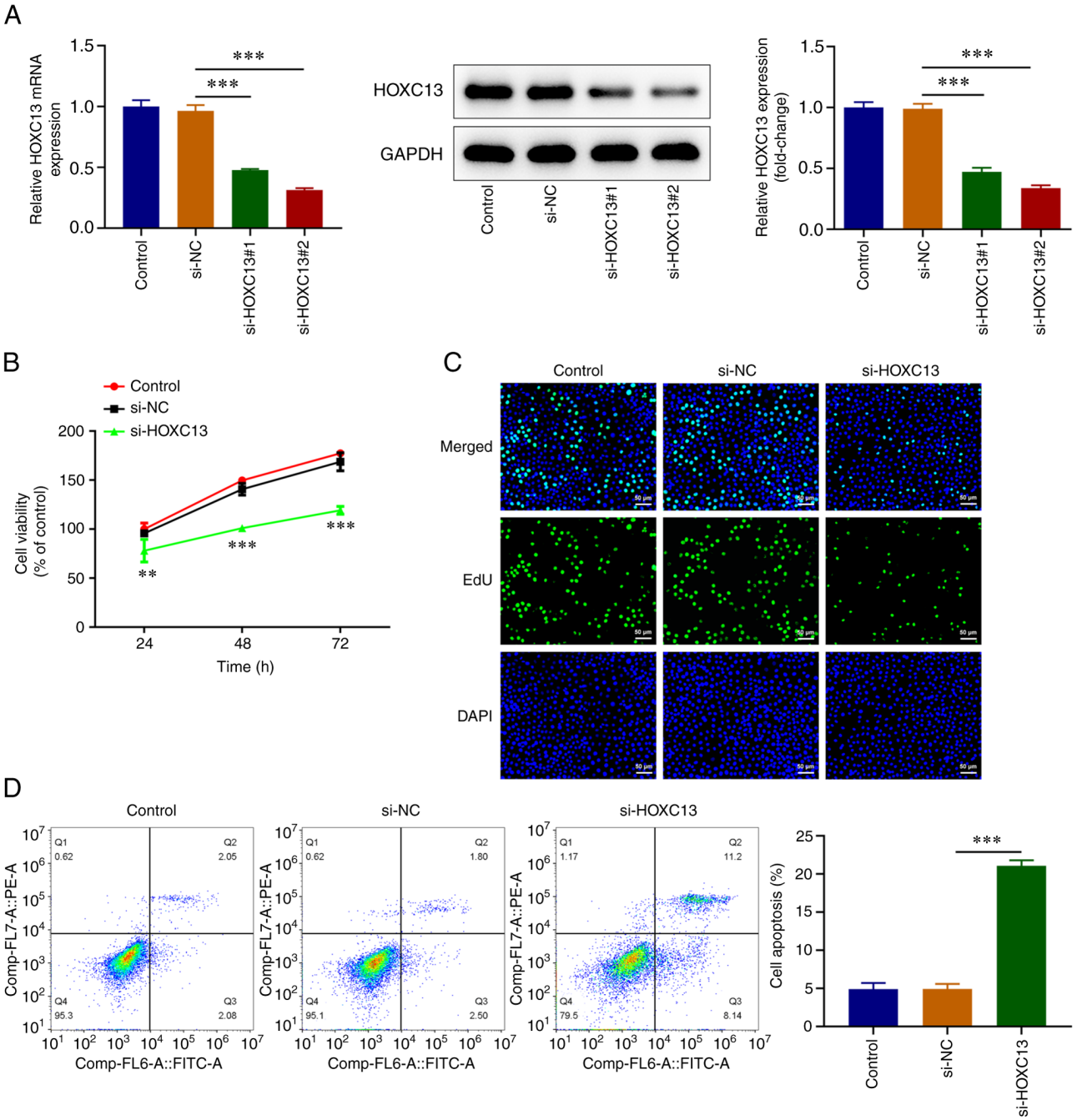

Figure 2. Interference with HOXC13 inhibits the viability, proliferation and induces apoptosis of breast cancer cells. (A) HOXC13 interference plasmid was constructed, and the transfection efficiency was detected by reverse transcription-quantitative PCR and western blot analysis. (B) Cell Counting Kit-8 assay detected cell viability. (C) EdU staining detected cell proliferation. (D) Flow cytometry detected apoptosis. **P<0.01 and ***P<0.001 vs. si-NC. HOXC13, homeobox C13; EdU, 5-ethynyl-2'-deoxyuridine; si, small interfering; NC, negative control.

performed via transfection, and efficiency was determined using RT-qPCR and western blot analysis. Transfection with si-HOXC13#1 and si-HOXC13#2 led to HOXC13 knockdown and transfection with si-HOXC13#2 led to the highest reductions in HOXC13 expression. Thus, si-HOXC13#2 was selected for subsequent experiments (Fig. 2A). The CCK-8 assay demonstrated that cell viability was significantly decreased in the si-HOXC13 group compared with that in the si-NC group (Fig. 2B). In addition, EdU staining revealed that cell proliferation was markedly decreased following HOXC3 knockdown (Fig. 2C). Flow cytometry demonstrated that apoptosis was significantly increased following HOXC13 knockdown (Fig. 2D). Overall, HOXC13 depletion obstructed the viability and proliferation while it stimulated the apoptosis of BC cells.

HOXC13 knockdown inhibits the migration, invasion and EMT of BC cells. Cell migration and invasion were measured using wound healing and Transwell assays. The results of the present study demonstrated that migration and invasion were significantly decreased in the si-HOXC13 group compared with that in the si-NC group (Fig. 3A and B). The expression

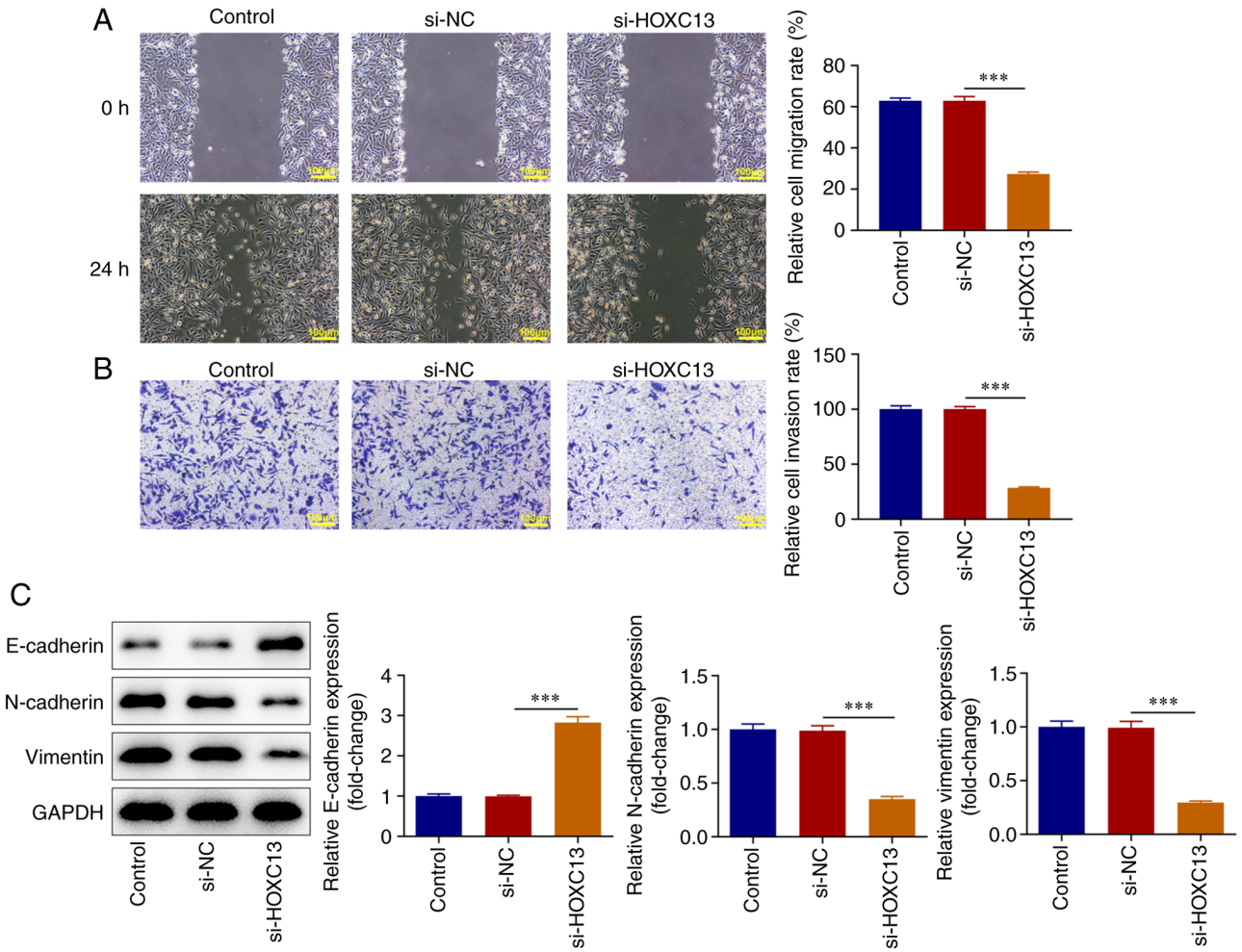

Figure 3. Interference with HOXC13 inhibits migration, invasion and EMT of breast cancer cells. Migration and invasion were measured by (A) wound healing and (B) Transwell assays (scale bar, 100 μm). (C) Expression levels of E-cadherin, N-cadherin and Vimentin were detected by western blot analysis. ***P<0.001. HOXC13, homeobox C13; si, small interfering; NC, negative control.

levels of epithelial-mesenchymal transition (EMT)-associated proteins, namely E-cadherin, N-cadherin and Vimentin, were detected using western blot analysis. The expression levels of E-cadherin were significantly increased in the si-HOXC13 group compared with those in the si-NC group, whereas the expression levels of N-cadherin and Vimentin were significantly decreased (Fig. 3C). To sum up, HOXC13 interference impeded the migration, invasion and EMT of BC cells.

HOXC13 knockdown inhibits glycolysis of BC cells. XF96 extracellular flux analyzer was used to detect ECAR. The results of the present study revealed that cell ECAR at 20-90 min were significantly decreased following HOXC13 knockdown (Fig. 4A). Moreover, lactic acid production (Fig. 4B), glucose consumption (Fig. 4C), and the expression levels of HK2 and PKM2 were significantly decreased (Fig. 4D) by HOXC13 knockdown. Accordingly, HOXC13 silencing impeded the glycolysis of BC cells.

HOXC13 positively regulates DNMT3A transcription in BC cells. The JASPAR database predicted the binding between HOXC13 and promoter sites of DNMT3A (Fig. 5A). RT-qPCR and western blot analysis revealed that DNMT3A expression was significantly increased in MDA-MB-231 cells compared with that in MCF-10A cells (Fig. 5B). Subsequently, the Oe-HOXC13 plasmid was constructed, and cells were divided into the Control, Oe-NC and Oe-HOXC13 groups. RT-qPCR and western blot analysis were used to detect transfection efficiency of HOXC13 overexpression plasmids and it was discovered that HOXC13 expression was significantly elevated following transfection of Oe-HOXC13 (Fig. 5C). The dual-luciferase and ChIP assays revealed that HOXC13 bound to the DNMT3A promoter in MDA-MB-231 cells compared with MCF-10A cells (Fig. 5D and E). RT-qPCR and western blot analysis demonstrated that DNMT3A expression was significantly increased in the Oe-HOXC13 group compared with that in the Oe-NC group. By contrast, DNMT3A expression was significantly decreased in the si-HOXC13 group compared with the si-NC group (Fig. 5F). Collectively, HOXC13 was a transcription activator of DNMT3A in BC cells.

HOXC13 regulates DNMT3A in malignant progression of BC. To investigate the mechanisms underlying HOXC13 regulation of the malignant progression of BC, an Oe-DNMT3A plasmid was constructed (Fig. 6A). Cells were divided into

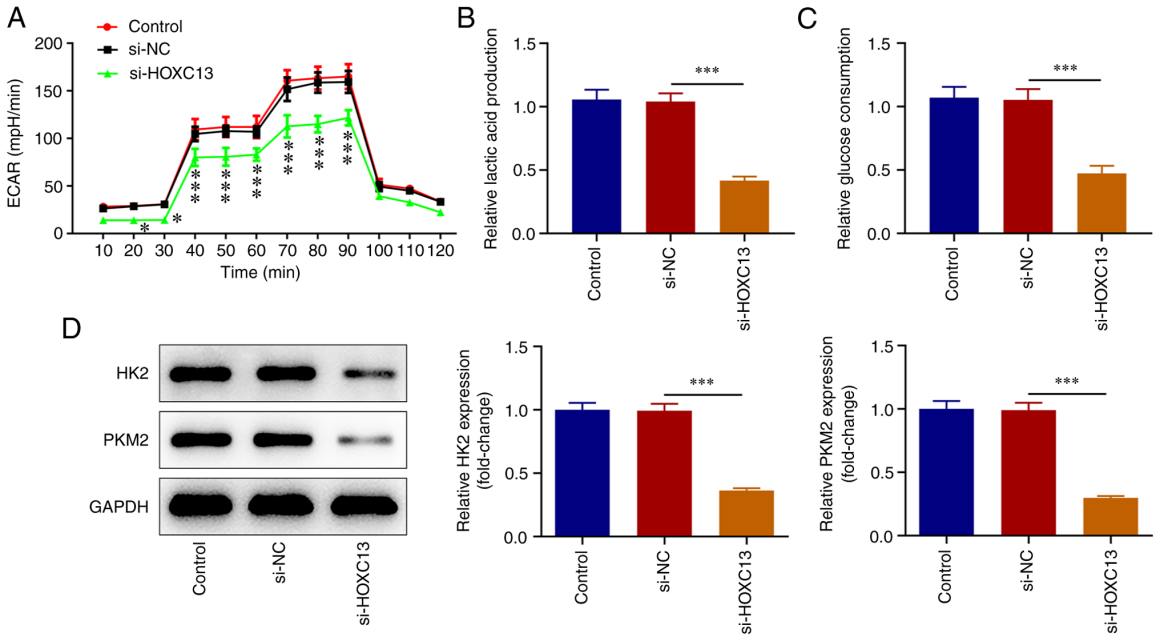

Figure 4. Interference with HOXC13 inhibits glycolysis of breast cancer cells. (A) XF96 extracellular flux analyzer detected ECAR. Kits measured (B) lactic acid production and (C) glucose consumption. (D) Expression levels of HK2 and PKM2 were detected by western blot analysis. *P<0.05 and ***P<0.001 vs. si-NC or as indicated. ECAR, extracellular acidification rate; HOXC13, homeobox C13; si, small interfering; NC, negative control; HK2, hexokinase 2; PKM2, pyruvate kinase M2.

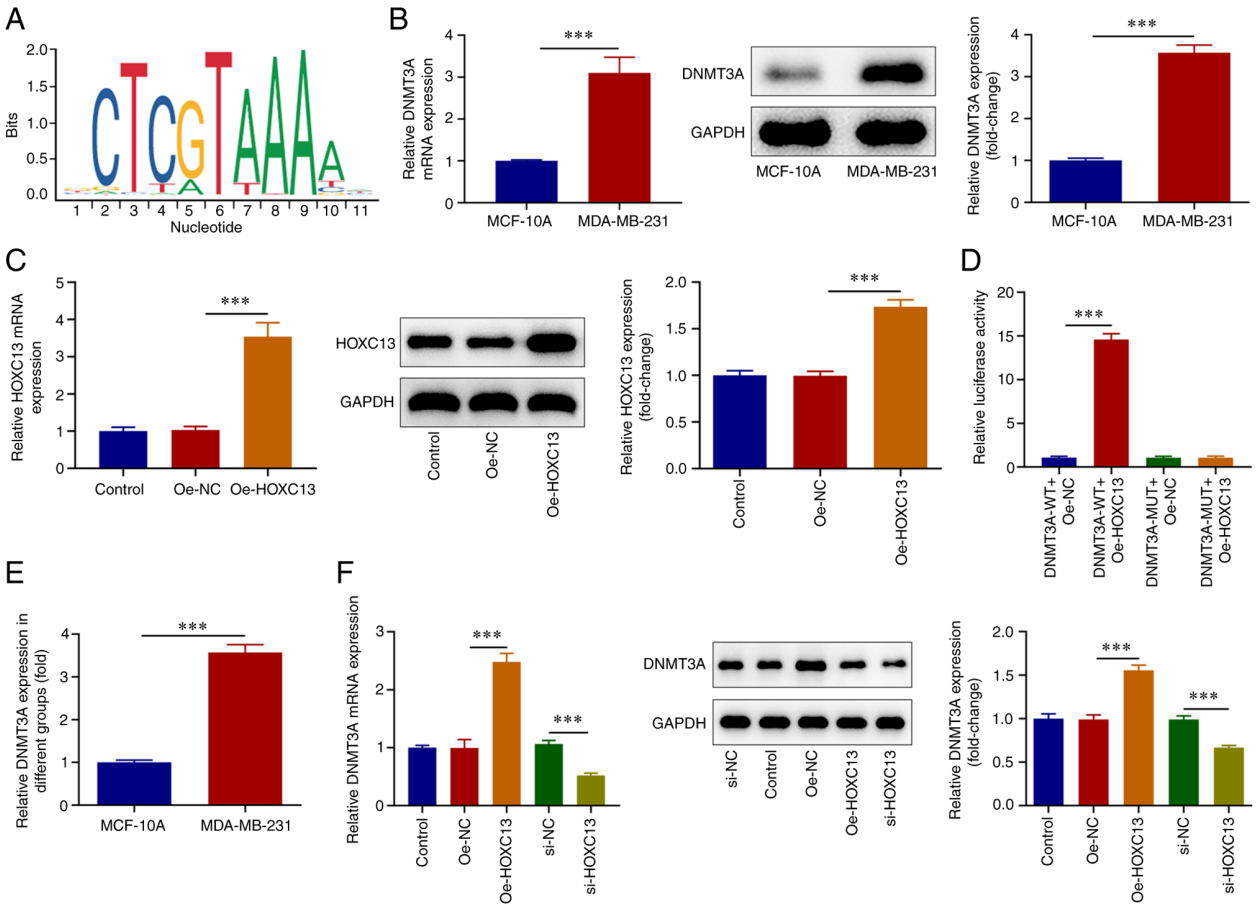

Figure 5. Transcription factor HOXC13 positively regulates DNMT3A transcription in breast cancer cells. (A) JASPAR database predicted the binding of transcription factor HOXC13 and promoter sites of DNMT3A. (B) RT-qPCR and western blot analysis showed that expression of DNMT3A was significantly increased in MDA-MB-231 cells. (C) RT-qPCR and western blot analysis were used to detect transfection efficiency. (D) Luciferase and (E) chromatin immunoprecipitation assay results showed HOXC13 binding to DNMT3A promoter. (F) RT-qPCR and western blot analysis detected expression of DNMT3A. ***P<0.001. HOXC13, homeobox C13; DNMT3A, DNA methyltransferase 3α; RT-qPCR, reverse transcription-quantitative PCR; Oe, overexpression; NC, negative control; si, small interfering; WT, wild-type; MUT, mutant.

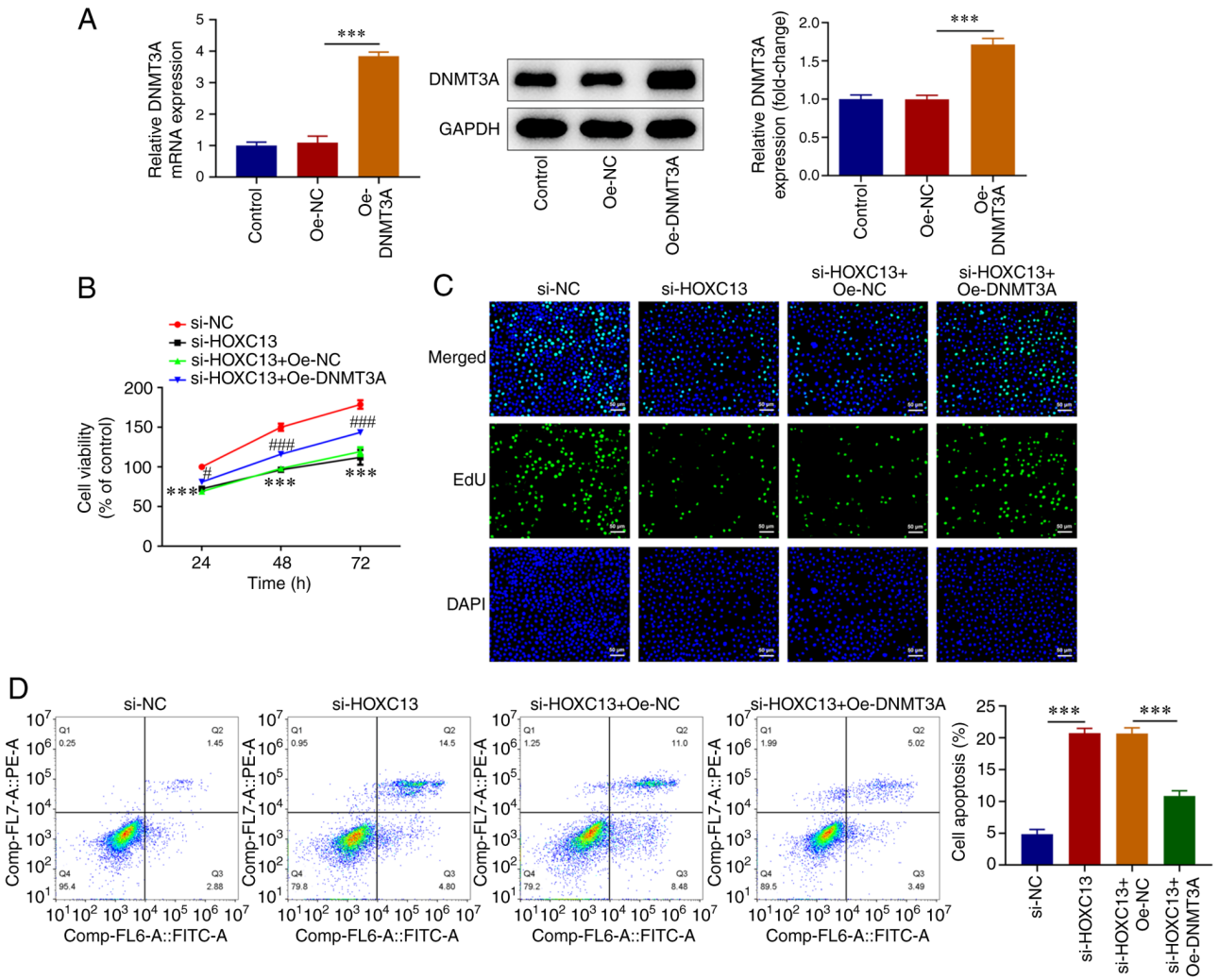

Figure 6. HOXC13 regulates DNMT3A in apoptosis of breast cancer cells. (A) Transfection efficiency of Oe-DNMT3A was detected by reverse transcription-quantitative PCR and western blot analysis. (B) Cell Counting Kit-8 assay detected cell viability. (C) EdU staining detected cell proliferation. (D) Flow cytometry detected apoptosis. ***P<0.001 vs. si-NC or Oe-NC; $^{\#}$P<0.05, $^{\#\#\#}$P<0.001 vs. si-HOXC13 + Oe-NC. HOXC13, homeobox C13; DNMT3A, DNA methyltransferase 3α; EdU, 5-ethynyl-2'-deoxyuridine; Oe, overexpression; NC, negative control; si, small interfering.

the si-NC, si-HOXC13, si-HOXC13 + Oe-NC and si-HOXC13 + Oe-DNMT3A groups. The CCK-8 and EdU assays demonstrated that cell viability was markedly increased in the si-HOXC13 + Oe-DNMT3A group compared with that in the si-HOXC13 + Oe-NC group (Fig. 6B and C). Flow cytometry revealed that apoptosis was significantly decreased in the si-HOXC13 + Oe-DNMT3A group compared with that in the si-HOXC13 + Oe-NC group (Fig. 6D). Wound healing and Transwell assays revealed that DNMT3A overexpression significantly reversed the inhibitory effects of HOXC13 knockdown on BC cell invasion and migration (Fig. 7A and B). Western blot analysis demonstrated that E-cadherin expression levels were significantly decreased, and N-cadherin and Vimentin expression levels were significantly increased in the si-HOXC13 + Oe-DNMT3A group compared with those in the si-HOXC13 + Oe-NC group (Fig. 7C). Results obtained using the XF96 extracellular flux analyzer demonstrated that in the si-HOXC13 + Oe-DNMT3A group, ECAR at 30-80 min, lactate levels (Fig. 8A and B), glucose consumption (Fig. 8C), and HK2 and PKM2 expression levels were significantly increased (Fig. 8D) compared with in the si-HOXC13 + Oe-NC group. Taken together, HOXC13 functioned in the aggressive behaviors of BC cells by regulating DNMT3A.

Discussion

Previous studies have demonstrated that HOXC13 is associated with the occurrence and development of hair and nails (21,22). Moreover, other studies have reported that HOX13 is significantly highly expressed in ameloblastoma, odontogenic tumor, melanoma and liposarcoma compared with healthy tissues (23-26). In addition, HOXC13 knockdown significantly inhibits the proliferation of colon cancer cells and induces cell cycle arrest (27). As a transcription factor, HOXC13 regulates the expression of numerous key genes, thus affecting the occurrence and development of tumors. Zinc finger protein 521, a proto-oncogene in B cells that causes leukemia, is co-regulated by HOXC13 (28). A previous study demonstrated that HOXC13 plays a role in promoting lung cancer via upregulation of cyclin D1 and cyclin E1 expression (29). Using the UALCAN database, the present study demonstrated that HOXC13 was highly expressed in patients with BC, and

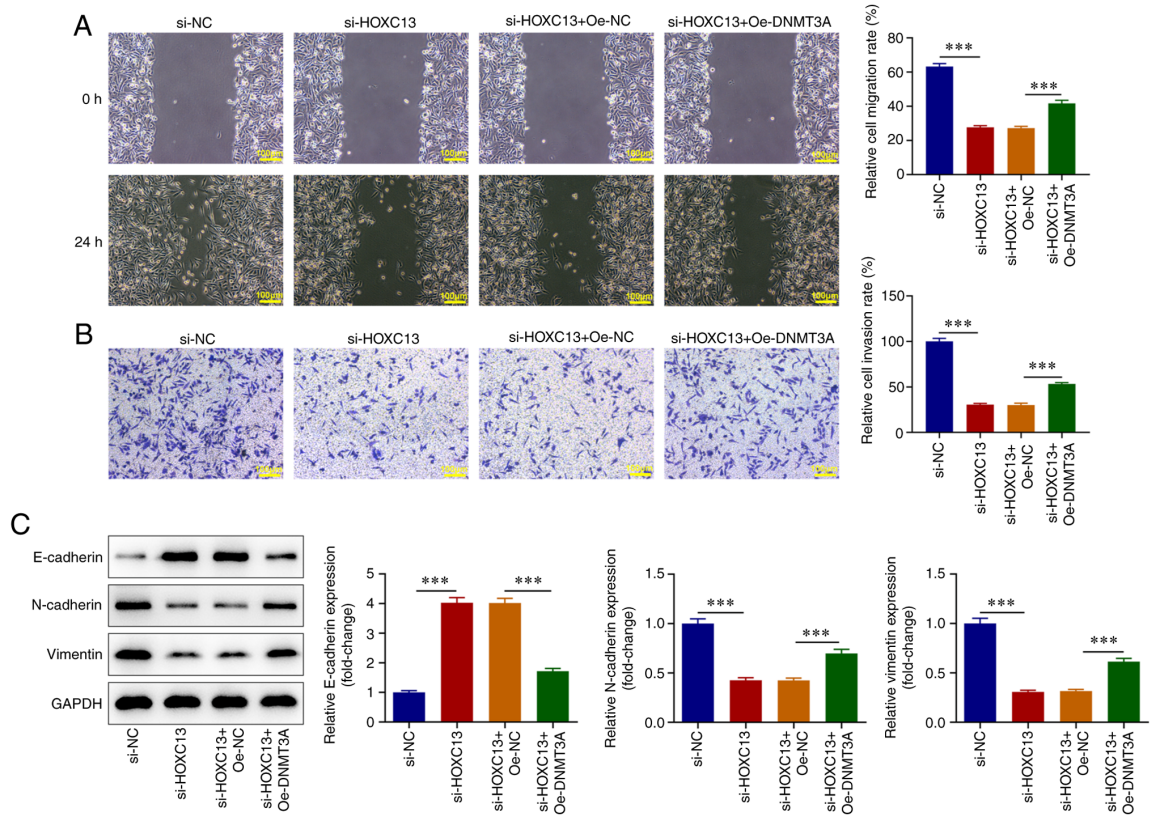

Figure 7. HOXC13 regulates DNMT3A in the invasion, migration and EMT of breast cancer cells. Migration and invasion were measured by (A) wound healing and (B) Transwell assays (scale bar, 100 μm). (C) Expression levels of E-cadherin, N-cadherin and Vimentin were detected by western blot analysis. ***P<0.001. HOXC13, homeobox C13; DNMT3A, DNA methyltransferase 3α; Oe, overexpression; NC, negative control; si, small interfering.

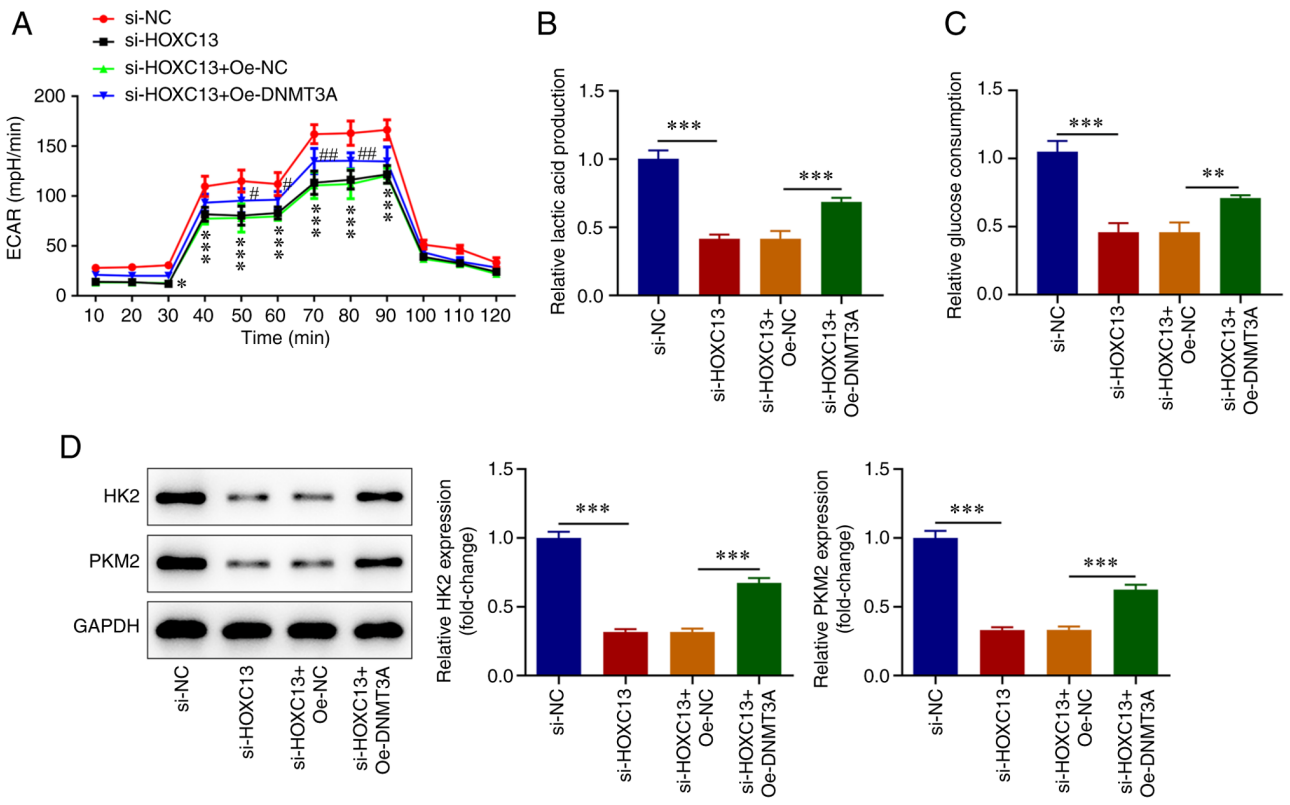

Figure 8. HOXC13 regulates DNMT3A in glycolysis of breast cancer cells. (A) XF96 extracellular flux analyzer detected ECAR. Kits were used to measure (B) lactic acid production and (C) glucose consumption. (D) Expression levels of HK2 and PKM2 were detected by western blot analysis. *P<0.05, **P<0.01 and ***P<0.001 vs. si-NC or si-HOXC13 + Oe-NC; $^{\#}$P<0.05 and $^{\#\#}$P<0.01 vs. si-HOXC13 + Oe-NC. HOXC13, homeobox C13; DNMT3A, DNA methyltransferase 3α; Oe, overexpression; NC, negative control; si, small interfering; ECAR, extracellular acidification rate; HK2, hexokinase 2; PKM2, pyruvate kinase M2.

this was associated with a poor prognosis and tumor staging of BC. Therefore, the present study aimed to determine the function and mechanism of HOXC13 in BC. BC and healthy mammary epithelial cells were used and the results were consistent with those predicted using the UALCAN database. Notably, the present study demonstrated that HOXC13 expression was significantly increased in BC cell lines. These results indicated the role of HOXC13 in BC; further investigations into the specific functions and mechanisms are required.

Results from UALCAN database in the current study demonstrated that HOXC13 was highly expressed in BC, and was associated with patient prognosis and tumor stage. Notably, cell proliferation, invasion and metastasis may be indicative of the malignant potential of tumors. Numerous studies have demonstrated that inhibition of the aforementioned functions may impact the malignant progression of tumor cells (30-32). In addition, glycolysis is a key metabolic characteristic of cells in the process of tumor development (33). Not only does glycolysis provide rapid energy for tumor cells, intermediate metabolites generated in the process are also crucial precursors for alternate metabolic pathways and glycolysis may provide raw materials for the synthesis of various biological macromolecules (34). Therefore, inhibition of aerobic glycolysis may be used in the clinical treatment of tumors. The present study demonstrated that the proliferation, invasion, migration and EMT of BC cells were decreased, and glycolysis was inhibited following HOXC13 knockdown. These results indicated that HOXC13 serves a role in promoting BC; further investigations into the specific mechanisms are required.

Transcription factors serve a key role in tumor development. The covalent binding domains of transcription factors and DNA either inhibit or enhance gene transcription (35). As a member of the HOX gene family, HOXC13 contains homologous domains that facilitate transcription factor functions (9). The promoter binding sites of transcription factors HOXC13 and DNMT3A were predicted using the JASPAR database. Moreover, the regulatory association between HOXC13 and DNMT3A in BC cells was verified using dual-luciferase reporter gene and ChIP assays. The present study demonstrated that DNMT3A expression was significantly increased in BC cell lines. A previous study demonstrated that lysine methyltransferase 2C deficiency promotes small cell lung cancer metastasis through DNMT3A-mediated epigenetic reprogramming (36). Moreover, DNMT3A epigenetically regulates key microRNAs (miRs) involved in EMT in prostate cancer (37). Ginsenoside 20 (S)-Rg3 that is identified as an active saponin monomer derived from red ginseng inhibits DNMT3A expression in SKOV3 ovarian cancer cells, reversing the DNMT3A-mediated methylation of the miR-532-3p host gene promoter. This subsequently increases miR-532-3p levels, and inhibits HK2 and PKM2 expression levels to inhibit the Warburg effect (26). The aforementioned results indicate that DNMT3A exerts a regulatory effect on tumor proliferation, metastasis and glycolysis. The present study demonstrated that DNMT3A overexpression in BC cells reversed the inhibitory effects of HOXC13 knockdown on the viability, proliferation, migration, invasion, EMT and glycolysis of tumor cells.

The present study had the limitation that it did not investigate the expression of HOXC13 in patients and animals with BC. In future, HOXC13 expression in patients with BC will be explored.

In conclusion, HOXC13 promoted cell viability, proliferation, migration, invasion, EMT and glycolysis in BC by regulating DNMT3A.

Acknowledgements

Not applicable.

Funding

No funding was received.

Availability of data and materials

The datasets used and/or analyzed during the current study are available from the corresponding author on reasonable request.

Authors' contributions

HL and LQ conceived and designed the study, analyzed data, and wrote and revised the manuscript. PG, HC, JZ, XZ, GL and LW performed the experiments. HL and LQ confirm the authenticity of all the raw data. All authors have read and approved the final manuscript.

Ethics approval and consent to participate

Not applicable.

Patient consent for publication

Not applicable.

Competing interests

The authors declare that they have no competing interests.

References

1. Katsura C, Ogunmwonyi I, Kankam HK and Saha S: Breast cancer: Presentation, investigation and management. Br J Hosp Med (Lond) 83: 1-7, 2022.
2. Sung H, Ferlay J, Siegel RL, Laversanne M, Soerjomataram I, Jemal A and Bray F: Global cancer statistics 2020: GLOBOCAN estimates of incidence and mortality worldwide for 36 cancers in 185 countries. CA Cancer J Clin 71: 209-249, 2021.
3. Chen W, Zheng R, Baade PD, Zhang S, Zeng H, Bray F, Jemal A, Yu XQ and He J: Cancer statistics in China, 2015. CA Cancer J Clin 66: 115-132, 2016.
4. Bose S and Le A: Glucose metabolism in cancer. Adv Exp Med Biol 1063: 3-12, 2018.
5. Shiraishi T, Verdone JE, Huang J, Kahlert UD, Hernandez JR, Torga G, Zarif JC, Epstein T, Gatenby R, McCartney A, *et al*: Glycolysis is the primary bioenergetic pathway for cell motility and cytoskeletal remodeling in human prostate and breast cancer cells. Oncotarget 6: 130-143, 2015.
6. Wu Z, Wu J, Zhao Q, Fu S and Jin J: Emerging roles of aerobic glycolysis in breast cancer. Clin Transl Oncol 22: 631-646, 2020.
7. Krumlauf R: Hox genes, clusters and collinearity. Int J Dev Biol 62: 659-663, 2018.
8. Ishii Y, Taguchi A and Kukimoto I: The homeobox transcription factor HOXC13 upregulates human papillomavirus E1 gene expression and contributes to viral genome maintenance. FEBS Lett 594: 751-762, 2020.

9. Li C, Cui J, Zou L, Zhu L and Wei W: Bioinformatics analysis of the expression of HOXC13 and its role in the prognosis of breast cancer. Oncol Lett 19: 899-907, 2020.
10. Luo J, Wang Z, Huang J, Yao Y, Sun Q, Wang J, Shen Y, Xu L and Ren B: HOXC13 promotes proliferation of esophageal squamous cell carcinoma via repressing transcription of CASP3. Cancer Sci 109: 317-329, 2018.
11. Liu B, Li J, Li JM, Liu GY and Wang YS: HOXC-AS2 mediates the proliferation, apoptosis, and migration of non-small cell lung cancer by combining with HOXC13 gene. Cell Cycle 20: 236-246, 2021.
12. Dai M, Song J, Wang L, Zhou K and Shu L: HOXC13 promotes cervical cancer proliferation, invasion and Warburg effect through β-catenin/c-Myc signaling pathway. J Bioenerg Biomembr 53: 597-608, 2021.
13. Okano M, Bell DW, Haber DA and Li E: DNA methyltransferases Dnmt3a and Dnmt3b are essential for de novo methylation and mammalian development. Cell 99: 247-257, 1999.
14. Yang X, Han H, De Carvalho DD, Lay FD, Jones PA and Liang G: Gene body methylation can alter gene expression and is a therapeutic target in cancer. Cancer Cell 26: 577-590, 2014.
15. Lu J, Zhen S, Tuo X, Chang S, Yang X, Zhou Y, Chen W, Zhao L and Li X: Downregulation of DNMT3A attenuates the warburg effect, proliferation, and invasion via promoting the inhibition of miR-603 on HK2 in ovarian cancer. Technol Cancer Res Treat 21: 15330338221110668, 2022.
16. Zhou Y, Yang Z, Zhang H, Li H, Zhang M, Wang H, Zhang M, Qiu P, Zhang R and Liu J: DNMT3A facilitates colorectal cancer progression via regulating DAB2IP mediated MEK/ERK activation. Biochim Biophys Acta Mol Basis Dis 1868: 166353, 2022.
17. Li Y, Jiang B, He Z, Zhu H, He R, Fan S, Wu X, Xie L and He X: circIQCH sponges miR-145 to promote breast cancer progression by upregulating DNMT3A expression. Aging (Albany NY) 12: 15532-15545, 2020.
18. Chandrashekar DS, Bashel B, Balasubramanya SAH, Creighton CJ, Ponce-Rodriguez I, Chakravarthi BVSK and Varambally S: UALCAN: A portal for facilitating tumor subgroup gene expression and survival analyses. Neoplasia 19: 649-658, 2017.
19. Fornes O, Castro-Mondragon JA, Khan A, van der Lee R, Zhang X, Richmond PA, Modi BP, Correard S, Gheorghe M, Baranasic D, *et al*: JASPAR 2020: Update of the open-access database of transcription factor binding profiles. Nucleic Acids Res 48(D1): D87-D92, 2020.
20. Livak KJ and Schmittgen TD: Analysis of relative gene expression data using real-time quantitative PCR and the 2(-Delta Delta C(T)) method. Methods 25: 402-408, 2001.
21. Wang S, Li F, Liu J, Zhang Y, Zheng Y, Ge W, Qu L and Wang X: Integrative analysis of methylome and transcriptome reveals the regulatory mechanisms of hair follicle morphogenesis in Cashmere Goat. Cells 9: 969, 2020.
22. Fernandez-Guerrero M, Yakushiji-Kaminatsui N, Lopez-Delisle L, Zdral S, Darbellay F, Perez-Gomez R, Bolt CC, Sanchez-Martin MA, Duboule D and Ros MA: Mammalian-specific ectodermal enhancers control the expression of Hoxc genes in developing nails and hair follicles. Proc Natl Acad Sci USA 117: 30509-30519, 2020.
23. Li J, Zhang B, Wang B and Zhang X: LncRNA HOXC-AS5 affects the proliferation, invasion and cell cycle of ameloblastoma cells by acting on the target gene HOXC13. Cell Mol Biol (Noisy-le-grand) 68: 124-134, 2022.
24. Hong YS, Wang J, Liu J, Zhang B, Hou L and Zhong M: Expression of HOX C13 in odontogenic tumors. Shanghai Kou Qiang Yi Xue 16: 587-591, 2007 (In Chinese).
25. Cantile M, Scognamiglio G, Anniciello A, Farina M, Gentilcore G, Santonastaso C, Fulciniti F, Cillo C, Franco R, Ascierto PA and Botti G: Increased HOX C13 expression in metastatic melanoma progression. J Transl Med 10: 91, 2012.
26. Cantile M, Galletta F, Franco R, Aquino G, Scognamiglio G, Marra L, Cerrone M, Malzone G, Manna A, Apice G, *et al*: Hyperexpression of HOXC13, located in the 12q13 chromosomal region, in well-differentiated and dedifferentiated human liposarcomas. Oncol Rep 30: 2579-2586, 2013.
27. Zhou Y, Zheng X, Lu J, Chen W, Li X and Zhao L: Ginsenoside 20(S)-Rg3 inhibits the warburg effect via modulating DNMT3A/MiR-532-3p/HK2 pathway in ovarian cancer cells. Cell Physiol Biochem 45: 2548-2559, 2018.
28. Yu M, Al-Dallal S, Al-Haj L, Panjwani S, McCartney AS, Edwards SM, Manjunath P, Walker C, Awgulewitsch A and Hentges KE: Transcriptional regulation of the proto-oncogene Zfp521 by SPI1 (PU.1) and HOXC13. Genesis 54: 519-533, 2016.
29. Yao Y, Luo J, Sun Q, Xu T, Sun S, Chen M, Lin X, Qian Q, Zhang Y, Cao L, *et al*: HOXC13 promotes proliferation of lung adenocarcinoma via modulation of CCND1 and CCNE1. Am J Cancer Res 7: 1820-1834. eCollection 2017, 2017.
30. Liu Z, Zhang L, Chen W, Yuan F, Yang Z, Liu S and Le F: miR-195-5p regulates cell proliferation, apoptosis, and invasion of thyroid cancer by targeting telomerase reverse transcriptase. Bioengineered 12: 6201-6209, 2021.
31. Fan C, Wang Q, van der Zon G, Ren J, Agaser C, Slieker RC, Iyengar PV, Mei H and Ten Dijke P: OVOL1 inhibits breast cancer cell invasion by enhancing the degradation of TGF-β type I receptor. Signal Transduct Target Ther 7: 126, 2022.
32. Fu Y, Zhang X, Liu X, Wang P, Chu W, Zhao W, Wang Y, Zhou G, Yu Y and Zhang H: The DNMT1-PAS1-PH20 axis drives breast cancer growth and metastasis. Signal Transduct Target Ther 7: 81, 2022.
33. Abbaszadeh Z, Cesmeli S and Biray Avci C: Crucial players in glycolysis: Cancer progress. Gene 726: 144158, 2020.
34. Abdel-Wahab AF, Mahmoud W and Al-Harizy RM: Targeting glucose metabolism to suppress cancer progression: Prospective of anti-glycolytic cancer therapy. Pharmacol Res 150: 104511, 2019.
35. Lambert M, Jambon S, Depauw S and David-Cordonnier MH: Targeting transcription factors for cancer treatment. Molecules 23: 1479, 2018.
36. Na F, Pan X, Chen J, Chen X, Wang M, Chi P, You L, Zhang L, Zhong A, Zhao L, *et al*: KMT2C deficiency promotes small cell lung cancer metastasis through DNMT3A-mediated epigenetic reprogramming. Nat Cancer 3: 753-767, 2022.
37. Mancini M, Grasso M, Muccillo L, Babbio F, Precazzini F, Castiglioni I, Zanetti V, Rizzo F, Pistore C, De Marino MG, *et al*: DNMT3A epigenetically regulates key microRNAs involved in epithelial-to-mesenchymal transition in prostate cancer. Carcinogenesis 42: 1449-1460, 2021.